

55875
101579

Experience Gained From Launch and Early Orbit Support of the Rossi X-Ray Timing Explorer (RXTE)*

D. R. Fink, K. B. Chapman, W. S. Davis, J. A. Hashmall,
S. E. Shulman, S. C. Underwood, and J. M. Zsoldos†
Computer Sciences Corporation
Lanham-Seabrook, Maryland, USA 20706

R. R. Harman
National Aeronautics and Space Administration
Goddard Space Flight Center
Greenbelt, Maryland, USA 20771

Abstract

This paper reports the results to date of early mission support provided by the personnel of the Goddard Space Flight Center (GSFC) Flight Dynamics Division (FDD) for the Rossi X-Ray Timing Explorer (RXTE) spacecraft. For this mission, the FDD supports onboard attitude determination and ephemeris propagation by supplying ground-based orbit and attitude solutions and calibration results. The first phase of that support was to provide launch window analyses. As the launch window was determined, acquisition attitudes were calculated and calibration slews were planned. Postlaunch, these slews provided the basis for ground-determined calibration. Ground-determined calibration results are used to improve the accuracy of onboard solutions. The FDD is applying new calibration tools designed to facilitate use of the simultaneous, high-accuracy star observations from the two RXTE star trackers for ground attitude determination and calibration. An evaluation of the performance of these new tools is presented in the paper. The FDD provides updates to the onboard star catalog based on preflight analysis and analysis of flight data. The in-flight results of the mission support in each area are summarized and compared with premission expectations.

1. Introduction

A background discussion of the Rossi X-Ray Timing Explorer (RXTE) and a description of the spacecraft attitude sensors are given in this section.

1.1 Background

RXTE is a three-axis stabilized inertially pointing spacecraft (mean of J2000.0 reference) with the goal of studying the time characteristics of astrophysical sources of x-rays. The mission is designed to study up to 20 science targets per day and to have a minimum lifetime of 2 years with a goal of 5 years. RXTE has no propulsion system and was built by GSFC Code 700.

RXTE was launched on December 30, 1995, by a Delta II launch vehicle into a 580-kilometer (km) circular orbit with a 23-degree (deg) inclination. The in-orbit checkout (IOC) phase began at separation from the Delta second stage and continued for approximately the first 30 days of the mission. During this phase, all the instruments were activated and tested. Also, various attitude maneuvers were performed to test the attitude control, power, and communications systems and to calibrate the science and attitude instruments.

* This work was supported by the National Aeronautics and Space Administration (NASA)/Goddard Space Flight Center (GSFC), Greenbelt, Maryland, under Contract NAS 5-31500.

† Currently at Orbital Sciences Corporation, Germantown, Maryland, USA, 20874

RXTE has the following power and thermal constraints during its mission (different constraints apply at Delta separation):

- The Sun must be in the +Z-hemisphere of the spacecraft (see Figure 1).
- The Sun must be within 5 degrees (deg) of the spacecraft XZ-plane to maximize power to the solar array and to prevent illumination of the spacecraft sides.
- The Sun must be further than 30 deg from the spacecraft +X-axis to prevent illumination of the star trackers and the science instruments.

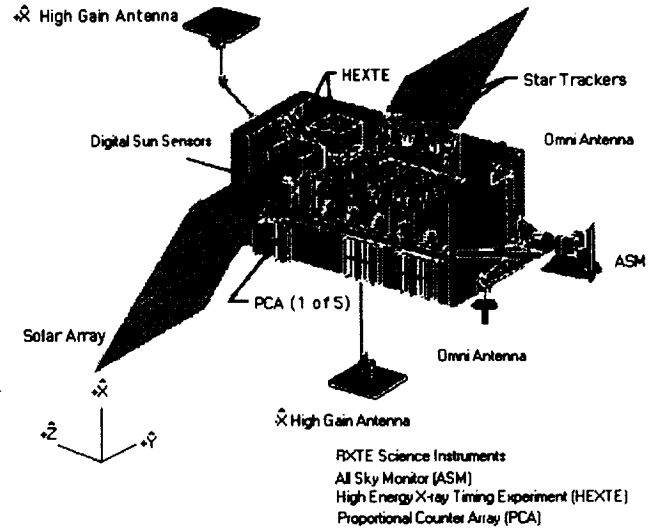


Figure 1. RXTE Spacecraft Diagram

The three-sigma attitude determination requirement on the RXTE onboard attitude system is 60 arc seconds (arc sec) around the X-axis and 42 arc sec each around the Y- and Z-axes. RXTE's attitude sensors and actuators are as follows:

- Two charge-coupled device (CCD) star trackers (STs)
- Eight coarse Sun sensors (CSSs)
- Two digital Sun sensors (DSSs)
- Two three-axis magnetometers (TAMs)
- One inertial reference unit (IRU) (three two-axis mechanical gyroscopes)
- Magnetic torquer bars (MTBs)
- One interferometric fiber optic gyroscope (IFOG), as an experiment
- Reaction wheel assembly (RWA)

1.2 Spacecraft Attitude Sensors

The RXTE STs are Ball Aerospace CT-601 CCD star trackers. They have an instrumental magnitude limit of 5.9, a field of view (FOV) of nominal dimension 8x8 deg, a noise equivalent angle of less than 3 arc sec (1σ), systematic position errors less than 3 arc sec, a magnitude uncertainty of 0.25, and a resolution of 0.5 arc sec. Each tracker can simultaneously track up to five stars. For specified performance, the Sun must be at least 30 deg from the boresight, the Moon must be at least 8 deg from the boresight, and the lit Earth must be at least 17.9 deg from the boresight. For RXTE, the boresight of ST1 nominally coincides with the spacecraft X-axis. The ST2 boresight is 9.9 deg from the spacecraft X-axis toward the Z-axis. The STs are rotated by 45 deg around each boresight, and their FOVs overlap by about 1 square deg. The onboard star catalog (OSC) used by the onboard computer (OBC) has 2844 stars in the range of 1.0 to 6.5 instrumental magnitude (instrumental magnitude corresponds to visual magnitude for a star of the same color as the Sun—for red stars it can be as much as two magnitudes brighter) and covers the sky with no “holes.” This means that an ST will see at least one star in the catalog for any pointing direction. A new catalog is being prepared to eliminate those stars between magnitude 5.9 (the actual CCD detection limit) and 6.5 (the old catalog limit). This catalog does have small holes but these constitute no more than about 0.1 percent of the possible attitudes.

The RXTE digital Sun sensors are Adcole devices, which are functionally similar to sensors on other missions such as Gamma Ray Observatory (GRO), Upper Atmosphere Research Satellite (UARS), and Extreme Ultraviolet Explorer (EUVE). They have a FOV dimension of 64x64 deg, an approximate digital resolution of 15 arc sec, a noise of $\pm 1/2$ the digital resolution, and an accuracy of 60 arc sec within a 32-deg radius. The DSS1 boresight is

18 deg from the spacecraft Z-axis toward the X-axis, and the DSS2 boresight is 42 deg from the spacecraft Z-axis toward the -X-axis.

The RXTE inertial reference unit is the Kearfott SKIRU-DII and is functionally similar to the Teledyne DRIRU (Dry Rotor IRU)-IIs used on spacecraft such as GRO, UARS, and EUVE. It consists of three 2-axis gyroscopes, which provide six channels of rate information, two for each spacecraft body axis. The IRU axes are nominally aligned with spacecraft body axes. The IRU has a low-rate resolution of 0.1 arc sec/count and high-rate resolution of 1.6 arc sec/count. The prelaunch measured noise parameters for the IRUs are rate noise of 6.7×10^{-3} arc sec/sec^{1/2} and bias noise of 3.4×10^{-5} arc sec/sec^{3/2}.

The three-axis magnetometers were built by GSFC Code 700 and are nominally aligned with the spacecraft axes. They have a digital resolution of 0.293 mG/count and are used both in the spacecraft momentum control logic and as backup sensors.

The interferometric fiber optic gyroscope is an experimental device built by Honeywell, which provides three channels (X, Y, and Z) of rate information. Each channel consists of a coil of fiber optic cable with counter-propagating beams of light. The measured phase shift of these beams is proportional to the angular rate around the axis of the coil. On each channel, the incremental angle is measured at 0.250second (sec) time intervals. With a digital resolution of 2^{-36} radians per count, the data then has a scale factor of 3.34×10^{-9} deg/sec per count.

2. Prelaunch Activities

A discussion of the RXTE prelaunch activities, including launch windows, launch slips, and attitude planning, is given below.

2.1 Launch Windows

The RXTE launch window was determined by three constraints: the spacecraft +Z-axis had to be within 9 deg of the spacecraft-to-Sun vector at separation, the spacecraft had to separate during spacecraft day, and separation needed to occur before 0900 local time at the release longitude. These constraints led to an 88-minute (min) window starting at 1438 coordinated universal time (UTC) for the first RXTE launch attempt on December 10, 1995.

2.2 Launch Slips

The first four launch attempts were scrubbed due to high-level wind constraint violations. As a result, investigations began on opening up the launch window by 1 hour on each side. Both Code 700 Attitude Control System (ACS) engineers and FDD agreed that there were no major problems with opening up the launch window; but to verify the assumptions, a spacecraft independent validation and verification facility (SIVVF) simulation should be done. If launch occurred at the opening of the extended window, RXTE would be in darkness for more than 4 minutes and over 23 deg off the Sun line at separation. The simulation later showed the window could be widened safely. The fifth launch attempt was scheduled for the following day, December 18, too soon to open up the window, as the simulation results were not yet in hand. Therefore, launch was scheduled using the nominal launch window constraints. Approximately 15 minutes into the window, high level winds had lowered to within launch constraints, but at T-minus 2.5 seconds, there was a main engine cut off (MECO) due to a faulty liquid oxygen valve.

The sixth launch attempt was scheduled for 1347 UTC on December 29, 1995, using the extended launch window. Even with a launch window more than 3 hours wide, high-level winds also scrubbed this launch attempt. RXTE was finally launched on the seventh attempt at 1348 UTC on December 30, 1995.

2.3 Attitude Planning

For each launch opportunity, attitude planning consisted of two activities: (1) predicting separation and acquisition attitudes and (2) planning maneuvers for calibration of the attitude sensors. Because launch dates commonly slip many times, automating these activities as much as possible is desirable.

For each mission, the Delta project provides a document called *Detailed Test Objectives* (DTO), which gives the attitude of the second stage at the time it releases the spacecraft. This attitude is independent of the launch time because it is referenced to an inertial frame defined by the Earth and launch site at the time of launch. Thus, given

the alignment of the spacecraft with respect to the second stage, the location of the launch site, and the time of launch, the attitude of the spacecraft with respect to a mean of J2000.0 inertial coordinate system can be computed. After separation from the second stage, the spacecraft nulls any tip-off rates, deploys its solar arrays, and maneuvers its Z-axis to point toward the Sun. To obtain an approximate prediction of the attitude achieved by this process (the acquisition attitude), it was assumed that the Z-axis rotates from its direction at separation toward the Sun by the smallest rotation; i.e., around the direction perpendicular to both the Z-axis and the Sun. A MATLAB® (Reference 1) program was written to compute the separation and acquisition attitudes as a function of launch time and date. It also computes the angle between the Sun and the Z-axis at the separation attitude. The program computes these quantities at 1-minute intervals. Separation Z-axis-to-Sun angles of 9 deg or less define the original launch window, which typically lasted 80 to 85 minutes. This tool was also used to predict attitudes and Sun angles for the extended (200 minutes) launch windows.

A total of 28 attitude maneuvers on four days was planned to obtain calibration data for the attitude sensors (see Section 7, Attitude Sensor Calibration). These maneuvers were required to have continuous star coverage by the star trackers, a few minutes before, during, and a few minutes after each maneuver. The maneuvers were also required to exercise all axes of the gyroscope and move the Sun around in the FOV of the Sun sensors. The maneuvers were restricted by Sun angle limits for thermal and power constraints and by Earth and Moon interference of the star trackers. On previous missions, manually planning such maneuvers for each launch opportunity consumed much analyst time. With the goal of automating some of these processes, the RXTE planning was initially done in a coordinate frame defined by the Sun and the orbit normal with origin at the center of the Earth. The start and end of each maneuver were defined by attitudes in this frame and the orbit angles relative to the Sun. Maneuver scenarios could then be designed for continuous tracker coverage (avoiding Earth interference) while also satisfying Sun requirements and restrictions. For each launch opportunity, a program was run to convert the reference frame of each start and end attitude from the Sun/orbit-normal frame to an inertial mean-of-J2000.0 frame and to convert the start and end orbit angles relative to the Sun to date and time. Unfortunately, a single maneuver scenario was not sufficient to accommodate the Sun both above and below the orbit plane and to avoid Moon interference in all maneuvers for all dates. Thus, several scenarios were developed to accommodate various Sun and Moon configurations.

The RXTE launch had to be planned for 13 dates. The automated tools previously described significantly reduced the analyst workload and response time. The main lesson learned from these experiences was that an extra margin for lit Earth interference of the trackers should be applied to allow for attitude settling, delays in starting maneuvers, and larger-than-expected Earth interference limits.

3. Launch and Separation

The attitude acquisition and orbit for RXTE during launch and separation are described below.

3.1 Attitude Acquisition

The solar arrays were deployed within 1 minute after separation from the Delta. The original timeline called for the spacecraft then to maneuver its Z-axis to the Sun using the CSSs (CSS Sun acquisition mode). However, as a result of the extended launch window, the spacecraft was still in shadow after solar array deployment. When the spacecraft entered sunlight, the maneuver to the Sun line was nominal. The early mission Sun angle history is given in Figure 2. Key attitude events during the first 10 minutes after separation are summarized in Table 1. FDD was able to solve for attitude soon after sunlight entry. The ground Real-Time Attitude Determination System (RTADS) was able to provide an accurate attitude and IRU bias within 5 minutes after the initial star acquisition. At about 49 minutes from separation, the OBC started to use the DSS to maintain the spacecraft Z-axis pointing toward the Sun (DSS Sun acquisition mode). The RTADS attitude was used to initialize the OBC ACS by 2 hours, 20 minutes, after separation. At separation plus 3.4 hours, the OBC entered initial tracker hold mode where it used star tracker data to hold an inertial attitude. Unfortunately, after about 20 minutes (min), problems with the star trackers forced a return to the DSS acquisition mode (see Section 4, In-Flight Anomalies).

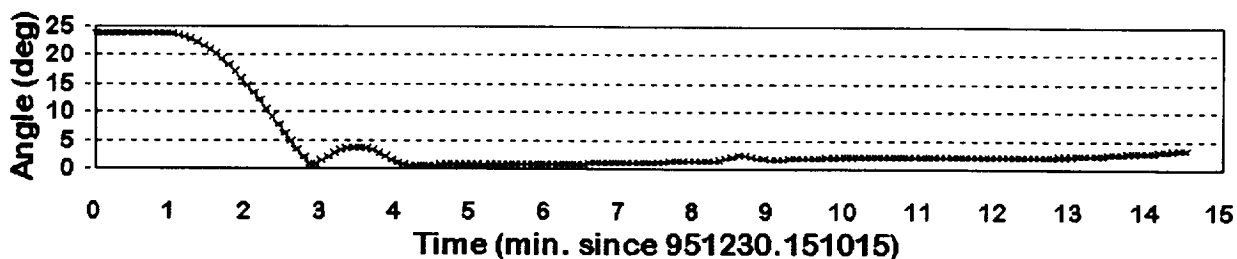


Figure 2. RXTE Z-Axis to Sun Angle Post Separation

Table 1. Key Separation Attitude Events

UTC (yymmdd.hhmmss)*	Separation + ΔT (min:sec)	Event
951230.150620	00:00	RXTE Separation from Delta-II: spacecraft +Z-Axis to Sun Angle = 23.970° Attitude (3-2-1): Yaw = 169.369° Pitch = -14.999° Roll = -106.399°
951230.150723	01:03	First valid CCD observation
951230.150800	01:40	Solar array deployment
951230.151105	04:45	Spacecraft enters daylight and starts maneuver to sunline
951230.151111	04:51	First valid DSS-2 observation
951230.151223	06:03	First valid DSS-1 observation
951230.151435	08:15	Maneuver to sunline complete: spacecraft +Z-Axis to Sun Angle = 0.610° Attitude (3-2-1): Yaw = -167.929° Pitch = -6.094° Roll = -113.916°

* yymmdd.hhmmss = year, month, day.hour, minute, seconds

3.2 Orbit

The RXTE orbit injection was close to nominal. Table 2 lists the nominal best estimated trajectory (BET), supplied prelaunch by McDonnell Douglas, and gives the differences from that nominal state from the redundant inertial flight control avionics (RIFCA) telemetry for second engine cut off II (SECO-II) at SECO-II epoch, which was 145850 Zulu (Z) (Zulu time is equivalent to UTC) on December 30, 1995. It also compares the BET at two epochs with the first operational FDD orbit solution computed using TDRS tracking data, E4.

Table 2. RXTE Orbit Injection State, Nominal Versus Actual

Parameter	Units	BET Orbit State	Δ BET to SECO-II	Δ BET to E4 at 1500Z	Δ BET to E4 at 1930Z
X	km	-4191.8098	-24.5395	-28.4313	-57.4932
Y	km	5553.1506	-18.2510	-27.3535	29.1369
Z	km	63.0661	12.2428	16.2096	13.1289
XDOT	km/sec	-5.54439	0.0215	0.0289	-0.0296
YDOT	km/sec	-4.21984	-0.0288	-0.0349	-0.606
ZDOT	km/sec	2.95639	-0.00047	-0.0015	0.0245
Semimajor Axis	km	6957.966	0.5091	-0.9563	-0.9304
Eccentricity		0.0001129	0.00001	-0.00014	0.000016
Inclination	deg	22.99837	-0.0016	-0.0018	-0.0015
Argument of Perigee	deg	88.3213	-20.4621	-13.0053	8.3147
R. A. Asc. Node*	deg	125.823	0.0142	0.0068	0.0054
True Anomaly	deg	273.0080	20.7202	13.3500	-7.7780
Period	min	6.2683	0.0106	-0.0199	-0.0193

* R. A. Asc. Node = right ascension of the ascending node

4. In-Flight Anomalies

In-flight anomalies for the RXTE mission included encounters with debris, star tracking problems, onboard computer/extended-precision vector (OBC/EPV) problems, and solar array power degradation. These anomalies are discussed in the following subsections.

4.1 Debris

Shortly after launch, it became apparent that there was some debris in the proximity of RXTE. This debris was of interest due to potential interference with the operation of RXTE sensors, as well as the possibility of collision. Later, when the prospect of collision seemed unlikely, this interest turned to the possibility of determining the origin and nature of the debris.

FDD requested and received unclassified North American Air Defense Command (NORAD) vectors and two-line elements for the debris. These types of elements are guaranteed by NORAD to be accurate within 5 km at their epoch. The elements were propagated into ephemerides. Ephemeris data were also generated to represent RXTE and Delta trajectories resulting from the SECO events (SECO-1, -2, -3, and -4) from the RIFCA data. The NORAD ephemerides were then compared with the SECO ephemerides to determine whether origin and collision points might be established.

These comparisons support the premise that these objects may have originated from the Delta/RXTE flight paths. The comparison results from Object 23758 to the SECO-3 and SECO-4 trajectories are interesting in that the distance is small at a time close to Delta maneuvers. Similarly, Object 23759's close trajectory to the SECO-2/RXTE state suggests a common original trajectory. However, these data are not sufficient to determine the exact origin and nature of the debris.

4.2 Star Tracking Problems

Each ST can track up to five stars in one of two modes. It can track a star at a directed position in the FOV or it can map the FOV, following each star detected for a programmed time. Each of the potential stars in the FOV occupy a logical "slot" in the star tracker. After launch, all five slots were programmed to map mode. Once a satisfactory inertial attitude had been achieved, three or four of the slots (during different periods) were programmed to track stars and the other one or two were directed to map. It was noticed that the STs frequently stopped tracking stars that they had been directed to track. The ST manufacturer claims that the only circumstance in which this could occur was if an object, brighter than the star being tracked, passed through the ST FOV and passed close to the star position. The occurrence of these tracking terminations (or break tracks) seemed to be explained by debris passing through the ST FOV.

This hypothesis was supported by the observation that in some cases when break tracks occurred, one could see a sudden increase in star brightness coupled with motion of the tracked object that soon moved out of the FOV. Additional support came from the star tracks observed in the ground star identification process. During this process, the spacecraft attitude is used to convert ST observations into vectors in inertial space. Occasionally, these vectors changed systematically along an apparent trajectory. Similar behavior had previously been observed only when an ST was pointed toward the unlit portion of the Earth (tracking city lights). For RXTE in the early mission, these trajectories appeared even when the STs were pointed away from the Earth.

By day 21, when the calibration validation maneuvers occurred, some break track events were still occurring. It seems likely that debris caused some of the break track events in the initial days after launch, but that other unexplained break tracks persisted after the debris dispersed.

As a consequence of the unexpected break track events, the DSS acquisition period was extended while ACS engineers and FDD analysts investigated the problem. For that mode, DSS1 maintains pitch (Y-axis) and roll (X-axis) control, while the IRU controls around the yaw (Z-axis). Over several hours, a small gyro bias caused the spacecraft to drift significantly around the Z-axis. Later, when engineers were more confident about the ST operation, the OBC was again allowed to use the star trackers to control the attitude. However, the original OBC program would command the STs to search for and acquire star only after maneuvers or after the end of periods of Earth occultation. Consequently, during inertial periods when the trackers were not occulted by the Earth, stars acquired at the start of the period would be lost one by one. By the end of the unocculted period, few or no stars

remained to be tracked. The OBC was reprogrammed at FDD request to command an ST to reacquire dropped stars even during nonoccultation periods.

GSFC Code 700 personnel have analyzed 31 hours of ST data provided by the FDD. They found 40 loss of tracking (LOT) events. Of these events, they attribute 24 to interference with unknown moving objects (e.g. debris or other satellites). The other 16 LOT events remain unexplained.

4.3 OBC-EPV Related Problems

After the first tracking data solution and extended precision vectors (EPVs) were delivered, the RXTE EPV from the first tracking data solution was not uplinked. The Tracking and Data Relay Satellite (TDRS) -7 EPV had also not been refreshed as advised. These two events, combined with the Network Control Center (NCC) not updating with the proper current RXTE vectors for TDRS, led to a TDRS-7 pass that suffered poor lock. Updates to the vectors at NCC cured the problem mid-pass. At that point, the RXTE propagations of the old EPV differed from the correct ephemeris by approximately 97 km; the TDRS-7 compares were approximately 16 km. These EPVs were then refreshed.

4.4 Solar Array Power Degradation

The power output of the solar arrays is 17 percent lower than expected. GSFC Code 700 engineers attribute the loss to a manufacturer defect which cracks individual solar cells. The defect affects five of the six panels. Such cracking is aggravated by stresses in the arrays. Therefore, ACS engineers have taken the following steps to reduce thermal and dynamic stress:

- Reprogram the on-board software to accelerate the arrays slowly whenever they are repositioned
- During periods of inertial pointing, position the normal of the panels 45 deg from the Sun (instead of the nominal 0 deg) to reduce the maximum temperatures of the array components
- Limit the maximum rate of attitude slews to 6 deg/min (instead of the nominal 12 deg/min)

The 45-deg tilt does result in an even lower power output. However, if no further degradation occurs, the spacecraft will still be able to carry out its mission. The CSS eyes are mounted both on the spacecraft body and on the arrays. The onboard CSS algorithm assumes that the arrays directly face the Sun. The use of a 45-deg solar array tilt invalidates this algorithm.

5. Performance of Star Trackers

Star tracker magnitude calibration and noise and distortion for RXTE are described below.

5.1 Magnitude Calibration

The flight software (FSW) gets 10 data samples per second for each star. The RXTE Kalman filter only processes a star once per second. The FSW star data processing averages the magnitude counts of the ten samples to obtain C_{ave} for each star, and then applies the following counts-to-magnitude conversion: $m = k_S * \ln(C_{ave}) + k_B$, where k_S is a constant that is the same for both trackers. Its value is -1.085736 , which equals $-2.5/\ln(10)$. The parameter k_B was determined preflight by measuring a class A0V reference star in each tracker. The preflight observed magnitude counts, C_0 , yield the following bias values:

$$\text{Tracker 1: } k_B = 11.851 = 2.5 * \log_{10}(C_0) \quad C_0 = 54988 \text{ (Reference 2)}$$

$$\text{Tracker 2: } k_B = 11.887 = 2.5 * \log_{10}(C_0) \quad C_0 = 56835 \text{ (Reference 2)}$$

The on-orbit magnitude calibration solution for ST1 combined data from the day of launch, and from the DSS calibration, IRU calibration, and calibration validation maneuvers. There were 736 total stars in all batches, of which 275 were OSC stars. Of those 275 stars, 250 were accepted for magnitude calibration. The solution ST2 used the same data spans as for ST1. For ST2, there were 619 total stars in all batches, of which 259 were OSC stars. Of

those 259 stars, 244 were accepted for magnitude calibration. Table 3 shows the results. Note that k_s and k_B are known in the FSW as the variables MagColScale and MagColBias, respectively.

In conclusion, both star trackers' premission magnitude calibration constants were within 0.06 magnitude of the values determined on-orbit. The constants can continue to be refined as more flight data are accumulated.

Table 3. On-Orbit Magnitude Calibration Results

Tracker	Prelaunch k_B	On-Orbit k_B	Δk_B (On-Orbit-Prelaunch)
1	11.851	11.9097 \pm 0.0481 (3 σ)	0.0587
2	11.887	11.9148 \pm 0.0418 (3 σ)	0.0278

5.2 Noise and Distortion

To obtain a quantitative estimate of the effects of noise and distortion on the star tracker observations, consider the combined residuals for both axes of both trackers obtained from single-frame attitude determination. For each star observation, the residual is the absolute magnitude of the difference between the observed and catalog vectors, both in spacecraft body coordinates. Star observations during maneuvers were used to obtain information throughout the FOV. For each time frame of the residual computation process, an attitude is computed using the single-frame quaternion estimation (QUEST) method (Reference 3) with star observations at or near that time. Propagation over short time intervals is used to group the observations at a common time. Then, the root-mean-square (RMS) of the residuals from all the frames is computed. These residuals are consistently about 3.0 arc sec RMS. The following error sources affect the residuals computed in that manner: sensor noise, sensor FOV calibration errors, attitude error, sensor bias and alignment errors, star catalog position errors, and center of brightness position shifts due to nearby stars. Stars used for this process were restricted to have a catalog position uncertainty of less than 1 arc sec and a predicted center of brightness shift less than 1 arc sec. In reality, most of the catalog stars have an uncertainty much less than 1 arc sec. These residuals are normally computed at the end of the alignment calibration process (see the section on Calibration Methods). Because attitude and alignments are solved-for with the same data used to compute the residuals, the RMS residuals are statistically reduced relative to the sensor residuals due to other error sources. Using the number of measurements and the number of quantities solved-for with these measurements, the RMS residuals are adjusted to compensate for this reduction (Reference 4). Table 4 shows these results for calibration maneuvers done on four separate days.

Table 4. Star Tracker Residuals From Alignment Callibrations

Day of Mission / Type of Data	RMS Residuals (arc sec)	Number of Attitudes Solved-for	Number of Star Observations	Adjusted RMS Residuals (arc sec)
1 / inertial	2.91	162	756	3.54
5 / maneuver	3.01	4169	18266	3.71
6 / maneuver	3.12	4343	17916	3.91
21 / maneuver	3.13	2152	9359	3.87

The RMS systematic errors across the FOV of the star tracker are specified to be no greater than 3 arc sec per axis, and the RMS noise is specified to be no more than 3 arc sec per axis. Combining these two sources of errors for both axes yields 6 arc sec. The adjusted RMS residuals are well within the specified 6 arc sec limit for all three sets of maneuvers (see Table 4), even though the adjusted residuals still contain catalog errors and nearby star errors up to 1 arc sec each. Future analyses are planned to obtain separate noise and distortions for each axis of each star tracker.

6. OBC Performance

RXTE OBC performance results in the areas of attitude and orbit accuracy are described below.

6.1 Attitude Accuracy

The RXTE spacecraft attitude determination requirement during the mission phase is for accuracy better than 0.02 deg. Requirements for attitude knowledge are 60 arc sec for the spacecraft X-axis and 42 arc sec for the Y- and Z-axes (all values are 3σ) (Reference 5). Results were obtained using the Coarse/Fine Attitude Determination System (CFADS) batch least-squares attitude determination algorithm. Table 5 illustrates ground-versus-OBC computed attitudes and their residuals from the most recent data at the time of this printing.

Table 5. OBC-Versus-Ground Solutions From CFADS

Epoch	OBC Attitude (degrees)			Ground Attitude (degrees)			Residuals* (arcsec)		
960303.0147	79.229	-45.999	91.060	79.231	-45.997	91.061	5.130	0.083	-1.979
960304.0232	79.229	-45.996	91.438	79.228	-46.000	91.438	-1.285	0.110	7.228
960308.0124	40.199	-61.254	126.890	40.201	-61.255	126.886	5.533	0.219	0.465
960315.0127	14.202	-60.756	158.853	14.203	-60.755	158.850	-3.591	0.504	0.364
960319.0231	-129.893	57.143	-124.258	-129.888	57.139	-124.254	0.857	-0.244	-6.055

* Average values based on the entire span of data using MTASS Attitude Validation Utility.

6.2 Orbit Accuracy

The RXTE OBC propagates the position for itself and up to three TDRS. This propagation is based on EPVs that are uplinked to the spacecraft. Fresh EPVs for RXTE are uplinked daily; the TDRS vectors are uplinked once per week. At launch, three TDRSs were in use for RXTE: TDRS-4, TDRS-5, and TDRS-7. These were designated TDRS-East, TDRS-West, and TDRS-Spare, respectively. TDRS-7 was later dropped from the lineup.

As a result of the stationkeeping being performed on TDRS-4 and -5, it is possible to use center of box (COB) EPVs for uplink to RXTE. The position uncertainty for TDRS-4 and -5 COB is approximately 130 km, corresponding to about 0.25 deg antenna-pointing error at RXTE. This approach was agreed to by the Project and has eliminated the need to support maneuvers for those TDRS. For COB propagation to be used onboard, the propagation modeling for the OBC was modified to use a table of geopotential values, enabling the proper modeling to be used for each spacecraft. For COB TDRS, the geopotential modeling is zeroed out in the table for those TDRS. For the other propagations, a truncated JGM-2 model is kept in the table.

During a simulation prior to launch, FDD discovered that the COB modeling had mistakenly been put in the RXTE OBC for TDRS-7. Analysis predicted that the OBC-versus-ground ephemeris error would be approximately 180 km, which fell within acceptable antenna-pointing error limits. This was brought to the attention of the Project, and the decision was made to fly with the error.

Initial analysis simulating the onboard propagator with a more complete environmental model than the OBC indicated the RXTE orbit state propagation error was <4 km over 1 day at the beginning of mission, and under 30 km per day throughout the solar cycle. However, prelaunch tests with the actual OBC propagator in the SIVVF and RXTE itself showed RXTE state propagation errors within 12 km per day typically, and the COB TDRS propagation errors within 26 meters at all times. The non-COB TDRS propagations were expected to perform similarly to the RXTE propagation.

At about 2 hours after separation, the OBC-versus-ground ephemeris comparisons computed by RTADS were as displayed in Table 6. Note that the comparison for TDRS-7 is high. The TDRS-7 orbit had changed as the result of a momentum control maneuver, and the Mission Operations Center (MOC) was advised that a new TDRS-7 EPV needed to be uplinked. Shortly after this comparison, it was uplinked. Since then, the observed propagation comparison results have RXTE staying within 12 km over a day and the COB TDRS maintaining < 26 meters.

Table 6. OBC Propagated Positions Versus Ground Ephemeris on 95/12/30 at ~1645Z

Spacecraft	RXTE	TDRS-4	TDRS-5	TDRS-7
Comparison (meters)	605	23	24	6493

7. Attitude Sensor Calibration

The calibration requirements, strategy and maneuvers, methods, and results for the RXTE mission are described below.

7.1 Calibration Requirements

The FDD was required to produce the following attitude sensor calibration products for the early RXTE mission:

- ST alignments
- DSS alignments and FOV calibration
- IRU alignment, scale factor, and bias calibration
- TAM alignment, scale factor, and bias calibration

The alignments of all sensors were to be referenced to ST1, which means that the alignment of ST1 should be unchanged as a result of the calibration process.

For the OBC to identify stars properly, the relative alignment error between the star trackers must be less than 200 arc sec. Although experiences with previous missions (Reference 6) have shown alignment launch shifts for star trackers to be less than this limit, the ACS engineers wanted to be prepared for larger launch shifts. Thus, the FDD needed to be able to calibrate the star tracker alignments on mission day 1.

The RXTE OBC does not use star data to update the attitude during maneuvers. The attitude during maneuvers is determined by propagating the last star tracker-based attitude solution with IRU data. Thus, it is important to have an accurate calibration of the IRU alignment and scale factor.

7.2 Calibration Strategy and Maneuvers

All attitude sensors were running soon after separation (mission day 1) from the Delta second stage. During the first 3 hours after separation, the FDD used ST and IRU data during an inertial period to solve for attitude and IRU bias. These were uplinked to the OBC to initialize the ACS Kalman filter. Next, analysts obtained preliminary star tracker alignments with a method that is insensitive to IRU calibration errors. These alignments are constrained so that the ST1 alignment does not change and the ST2 alignment absorbs all of the alignment correction. These alignments were uplinked to the OBC and used in the FDD ground system.

On mission day 3, the spacecraft carried out a sequence of moderate-sized maneuvers (about 25 deg) to obtain ST and IRU data for a preliminary IRU alignment/scale factor calibration, also to be uplinked to the OBC and used in the FDD ground system. These maneuvers were designed to obtain rotation information about all three IRU axes. In this calibration, the IRU alignment is referenced to the STs.

On mission day 5, a sequence of large (48- to 175-deg) maneuvers was executed to obtain data for comprehensive ST alignment calibration and IRU alignment/scale factor calibration. These maneuvers give rotation information about all three IRU axes, and star observations before, during, and after each maneuver. Analysts used the ST data to obtain comprehensive star tracker alignments. Again, these alignments are constrained so that the ST1 alignment does not change. Then, these data were used to obtain a comprehensive alignment/scale factor calibration of the IRU. Again, these were uplinked to the spacecraft and used by the ground system.

On mission day 6, a sequence of large (49- to 122-deg) maneuvers was executed to obtain data for comprehensive alignment and FOV calibration of the DSSs. These maneuvers were designed to sweep the Sun through the entire FOV of both DSSs, consistent with Sun constraints. Using ST and DSS data, the DSSs were first aligned relative to the STs. Then, adjustments to the Sun's image within the FOV were made. These results were uplinked to the OBC and used by the ground system.

On mission day 21, another sequence of large (49- to 180-deg) maneuvers was executed to obtain independent data for validating the IRU and ST calibrations.

Any convenient interval of continuous data may be used for the magnetometer calibration. Day 5 data are being used for calibration of the IFOG.

7.3 Calibration Methods

The alignment calibration method for the star trackers and Sun sensors must be able to handle multiple star observations at one time from the star trackers and single object observations from the Sun sensors, and must also be able to digest such data coming at different times and rates. It is also necessary to have a method that produces results on mission day 1. Past experiences with in-flight calibration have shown gyroscope calibration to be lengthy with many complications. Thus, it is desirable to separate the alignment calibration of star trackers and Sun sensors from that of gyroscopes. Specifically, the ST/DSS alignment algorithm should be insensitive to gyroscope alignment/scale factor errors.

The chosen alignment algorithm computes attitude and alignment at the times of the observations of one of the star trackers, the *primary* sensor. Observations from the other star tracker and from the Sun sensors are made at different times. Using IRU data, the other sensor data are rotated to the attitudes at which the primary sensor observations are made. Because the time intervals over which these rotations are made are small, less than 1 sec, the error introduced by IRU alignment/scale factor error is negligible (less than 0.045 arc sec). At each such time, a new attitude is computed, while alignment adjustments are accumulated over all the times (Reference 7).

To model systematic errors in the gyroscopes, both in-flight and ground attitude systems compute the average angular rate $\bar{\omega}$ from IRU incremental angle counts $\Delta\bar{N}$ during time interval Δt with the following equation:

$$\bar{\omega} = G \begin{bmatrix} k_x \Delta N_x \\ k_y \Delta N_y \\ k_z \Delta N_z \end{bmatrix} \frac{1}{\Delta t} - \bar{b}$$

where G is the 3×3 alignment/scale factor matrix; k_x , k_y , and k_z are scale factors for each channel; and \bar{b} is the bias vector. FDD IRU calibration systems solve for a matrix M and a vector $\delta\bar{b}$, which are used to adjust the calibration parameters as follows: $G' = (I + M)G$ and $\bar{b}' = \bar{b} + \delta\bar{b}$. The elements of the matrix M are small and provide for adjustments to the scale factors as well as the alignment of each axis of the IRU. However, at inertial attitudes, alignment/scale factor errors are not observable; maneuvers are needed to distinguish them from the bias. Kalman filters onboard the spacecraft and in the ground system can accurately solve for attitude and IRU bias with ST and IRU data, but errors in the IRU alignment/scale factor matrix manifest themselves during attitude maneuvers. Several methods are available for calibration of the gyroscope. The Davenport gyroscope calibration algorithm (Reference 8) is used to solve for these errors. This algorithm compares attitudes before and after maneuvers to the rotation obtained by integrating IRU data for the same maneuvers. Initial and final attitudes are computed with inertial data to free them from alignment/scale factor errors. Maneuver data from RXTE mission days 3, 5, or 21 may be used for this calibration.

As an extension to the Davenport method with inertial attitudes, note that during the constant rate portion of maneuvers, an attitude determination algorithm that also solves for IRU bias can get an accurate attitude, independent of gyro alignment/scale factor error. Even though the IRU bias is corrupted by the IRU alignment/scale factor error, the attitude is accurately determined. Thus, the Davenport method may also be used with attitudes derived from constant rate data during maneuvers.

A successful method for calibrating the DSS FOV distortions in flight is documented by Hashmall (References 9 and 10). This method incorporates adjustments to the coefficients of the manufacturer-supplied calibration function with *additional adjustments* that account for a relative misalignment between the two heads of the DSS. The method requires an accurate attitude history obtained from ST and IRU data. This history is obtained from the DSS calibration maneuvers (mission day 6), where the Sun is swept across the FOVs of the DSSs. Using this history and the calibrated DSS alignments, the reference Sun vector, obtained from precision Sun ephemeris and corrected for

velocity aberration and parallax, is transformed into the Sun sensor coordinate frames and then used to compute angles within the FOV. The difference between these references and the observed Sun angles in the FOV is used to compute the corrections to the calibration coefficients using batch least squares methods.

As with the DSS FOV calibration, the magnetometer calibration relies on an accurate attitude history obtained from ST and IRU data. With this history, a model of the Earth magnetic field, and the spacecraft ephemeris, the reference Earth field is transformed to body coordinates and compared with the magnetic field computed from magnetometer measurements and adjusted for bias and magnetic torquer effects. Using a batch least squares method, the differences between the two fields are used to compute adjustments to the magnetometer bias, alignment, scale factors, and torquer-to-magnetometer coupling matrix.

7.4 Calibration Results

Because ST1 is used as a reference sensor (its alignment is kept fixed), the change in the ST2 alignment is equal to the change in the relative alignment between the two sensors. Table 7 summarizes the results of four alignment calibrations. The table shows the change in relative alignments with respect to the prelaunch alignments.

Table 7. ST-Callbrated Relative Alignment Adjustments

Type of Data	X-Axis (arc sec)	Y-Axis (arc sec)	Z-Axis (arc sec)
Day 1 Inertial	-27.66	-15.18	2.37
Day 5 Maneuver	-24.24	-18.05	1.36
Day 6 Maneuver	-28.40	-17.69	3.13
Day 21 Maneuver	-24.44	-17.05	2.10

These relative alignment change results are also plotted in Figure 3. Table 5, in Section 5, shows the amount of data that was used for each of these solutions.

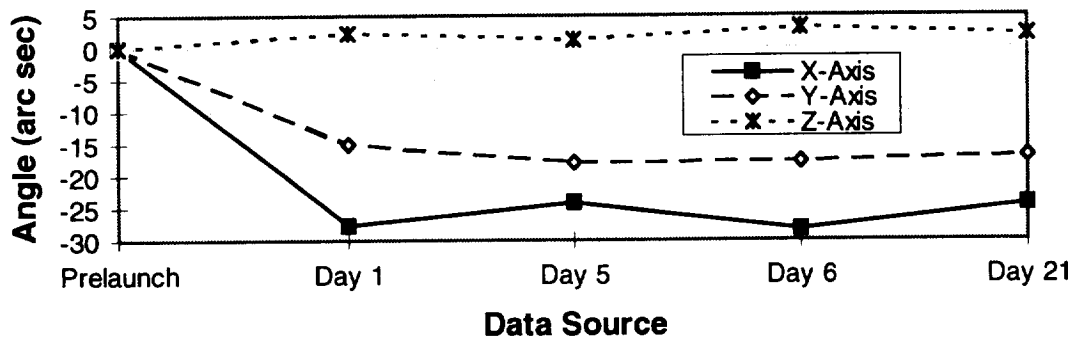


Figure 3. RXTE ST1/ST2 Relative Alignment Results

To obtain an idea of the uncertainty of the ST alignment calibration results, a separate ST alignment calibration was done for each of the nine maneuvers on mission day 6. The alignment calibration of that day is a weighted sum of the results of each individual maneuver. The dispersion of these individual solutions indicates the uncertainty of the weighted sum. The empirical 1σ uncertainties for the day 6 solution are 5.1, 0.4, and 1.3 arc sec for the X-, Y-, and Z-axes, respectively.

The relative ST alignment calibration data show some interesting results. The relative alignment fluctuations around the X-axis are greater than the other two axes. This behavior is expected, because the relatively small FOV of the trackers (± 4 deg) results in higher rotational errors around their boresights, and because the ST1 boresight is aligned

along the body X-axis, and the ST2 boresight is less than 10-deg from the body X-axis. An important result is that the relative alignment between ST1 and ST2 is stable from day to day. In particular, the fluctuations of calibrations of mission days 5, 6, and 21, which use relatively large amounts of data, are consistent with the day 6 empirical uncertainty. Another interesting point is that the calibration of mission day 1, which used much smaller amounts of data (see Table 4), is very close to the other calibrations.

Table 8. Bias Solutions for Low-Rate Primary IRU Channels

Data and Processing	X-Axis (deg/hr)	Y-Axis (deg/hr)	Z-Axis (deg/hr)
Prelaunch	-0.1916	-1.0165	0.7144
Day 1 CFADS	-0.2319	-1.1042	0.8121
Day 3 IRUCAL for Preliminary Calibration	-0.2282	-1.0984	0.8101
Day 5 CFADS	-0.2224	-1.1023	0.8072
Day 6 CFADS	-0.2341	-1.1022	0.8068
Day 21 IRUCAL for Calibration Validation	-0.2292	-1.0989	0.8059

Table 8 summarizes a few of the many IRU bias solutions obtained using two different software packages. The CFADS is a batch least squares processor, used to solve for attitude and IRU bias using ST and IRU data. The IRU calibration system (IRUCAL) implements the Davenport gyroscope calibration algorithm and was used to solve for both IRU bias and the alignment/scale factor matrix. As seen in Table 8, both methods give consistent results that were stable over the early mission. Figure 4 presents the bias changes graphically. In this figure, the bias is expressed relative to the prelaunch value. On some other missions, IRU biases drifted over the first few days after launch (Reference 6)]. On RXTE, this effect was not seen.

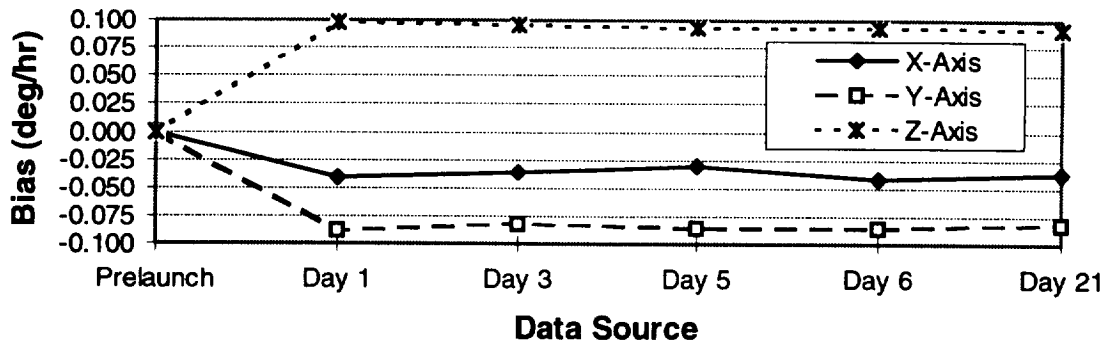


Figure 4. RXTE IRU Bias Relative to Prelaunch

In addition to CFADS and IRUCAL, the FDD ground system also computed an IRU bias using two Kalman filters, one running in real time (RTADS) and another running off-line (FILTER). The IRU bias for all four systems was consistent with each other and with the bias from the OBC Kalman filter.

Adjustments to the IRU alignment/scale factor matrix are given by the matrix M (see Section 7.3, Calibration Methods). The components of this matrix correct for the propagation error in each direction per angle rotated for each axis of rotation. These components are dimensionless, but can be interpreted to have the units “radians of propagation error per radian of rotation.” The diagonal components of the matrix M provide adjustments to the scale factor of each axis, because they give propagation errors along the direction of rotation. Whereas, the off-diagonal components provide propagation errors in the directions perpendicular to the rotation axes. The off-diagonal components also give alignment errors of the IRU axes. This dual interpretation occurs because a misalignment will cause a body axis rate to project a small amount onto the incorrect IRU axis, leading to the propagation error. It is

convenient to express this matrix in the units “arc sec of propagation error per radian of rotation,” which also gives alignment errors in arc sec.

Some of the results of the IRU calibration effort are given in Table 9. Alignment/scale factor adjustments are given relative to the prelaunch calibration. IRU alignments and scale factors obtained from the adjustments of the first and last solutions in Table 9 were delivered for use in the OBC and in the ground system. Analysts experienced difficulty in processing the IRU data for calibration, especially the day 5 data. Data gaps, particularly during the acceleration segments of maneuvers, complicated the analysis. Improved methods for handling such gaps and algorithms that do not require rate data at evenly spaced intervals will be used in future missions.

Table 9. Results of IRU Alignment/Scale Factor Calibration

Method	Davenport Algorithm With Inertial Attitudes			Davenport Algorithm With Rotating Attitudes			Davenport Algorithm With Inertial Attitudes		
Data	Day 3 Preliminary Calibration Maneuvers			Day 5 IRU Calibration Maneuvers			Day 21 Calibration Validation Maneuvers		
<i>M</i> (arc sec/rad)	-19.20	30.20	-7.75	-0.03	6.40	-19.57	-1.01	18.39	-24.54
	-24.10	-8.33	-39.36	6.97	-14.42	-54.33	-0.23	-18.22	-57.54
	28.88	44.63	-16.13	27.00	44.72	-10.46	28.59	46.31	-4.39

FDD analysts used data from the mission day 6 maneuvers to calibrate the DSS alignments with respect to the star trackers. The alignment adjustment around each axis of each sensor is given in Table 10. These adjustments are relative to the prelaunch alignments and are expressed in body coordinates.

Table 10. DSS Alignment Adjustments

Sensor	X-Axis (arc sec)	Y-Axis (arc sec)	Z-Axis (arc sec)
DSS1	-54.27	166.99	-25.86
DSS2	17.12	26.14	-49.30

The DSS FOVs were also calibrated with data from mission day 6 maneuvers, improving the residuals as indicated in Table 11. Separate residuals are given for each of the two angles, α and β , in the FOV. Because the Sun is constrained to be within 5 deg of the RXTE XZ-plane, the total variation in β is ± 5 deg at the center of each FOV, and ± 5.890 deg at the edge of the FOV. The α angle is allowed to vary over its full ± 32 -deg range. For this reason, the DSS FOV calibration must fit the data over a smaller portion of the β range than the α range. The initial FOV calibration residuals are smaller

Table 11. DSS FOV Calibration Residuals

Residuals	Initial (arc sec)	Final (arc sec)
DSS1 α	20.67	18.42
DSS1 β	18.14	9.70
DSS2 α	24.21	22.97
DSS2 β	14.41	8.51

than the initial residuals of the Sun sensors of other missions. This behavior is attributed to the restricted DSS FOV for RXTE. The final residuals after calibration are smaller for β than for α , because the smaller range of β contains less systematic variations than the full ± 32 -deg range. Were it not for the constraint on β , a more accurate fit could be obtained. However, as long as β remains small, any deficiency in the fit cannot be observed.

At the time this paper was written, the magnetometer calibration was still preliminary. FDD analysts have succeeded in obtaining improved calibration parameters, which reduce the error of attitude solutions using only TAM and IRU data from 0.5 deg to 0.2 deg per axis (1σ). However, systematic errors are still evident in the residuals. For previous similar missions, such errors have been reduced to less than 0.07 deg per axis (1σ). Analysts are investigating inconsistencies in the processing.

8. Conclusions

RXTE launch and in-orbit checkout support by the FDD was successful despite the anomalies encountered. The FDD was able to provide the orbit and attitude state vectors and the calibration information to the RXTE Project that were needed to transition the RXTE spacecraft into its operational phase. The most serious anomalies occurred with the CCD star trackers. Although they are superb attitude instruments, the debris and dropped star problems show they, nonetheless, are capable of strange behavior. Future flight software and FDD support procedures must be designed with these experiences in mind.

Acknowledgments

A few of the many other people who contributed significantly to the FDD's RXTE effort since its inception in 1992 are listed alphabetically below:

David Bolvin	James Cappellari	David Green	Leeann Lindrose	Joseph Sedlak
Robert Boyer	Lynn Carlson	Tom Gwynn	Chad Mendelsohn	David Shoup
Dan Brasoveanu	Murty Challa	James Heimerl	Douglas Moore	Mark Summerfield
Len Brockman	Donald Chu	Vilas Johnson	Neil Ottenstein	Susan Ray Valett
Evette Brown-Conwell	Orville Filla	Jon Landis	Anthony Paola	Scott Wallace
Alexander Calder	Jonathan Glickman	Michael Lee	Robert Rashkin	

The authors also acknowledge valuable conversations with Joseph Whitacre, Michael Femiano, Kong Ha, and Lou Hallock, and express their gratitude to the entire Flight Operations Team for the excellent teamwork.

References

1. The MathWorks, Incorporated, *MATLAB High-Performance Numeric Computation and Visualization Software, Reference Guide*. Natick, Massachusetts: The MathWorks, October 1992 (and reprints July 1993, September 1994, April 1995)
2. P. Newman, Swales & Associates, Inc., electronic memorandum, *GOV_IP.MCD*, September 15, 1994
3. M. Shuster and S. Oh, "Three-Axis Attitude Determination from Vector Observations," Paper No. AIAA 81-4003, *J. Guidance and Control*, Vol. 4, No. 1, January-February 1981, p. 70
4. W. Press, B. Flannery, S. Teukolsky, and W. Vetterling, *Numerical Recipes in C, The Art of Scientific Computing*, 2nd ed. Cambridge: Cambridge University Press, 1995, p. 662
5. Goddard Space Flight Center, *Detailed Mission Requirements--Issue 2 (DMR-2) Final Draft for the X-ray Timing Explorer (XTE)*, S. Coyle and J. Joyce, April 1993
6. W. Davis, J. Hashmall, J. Garrick, and R. Harman, "Postlaunch Calibration of Spacecraft Attitude Instruments," Paper No. AAS 93-325, *Spaceflight Dynamics 1993, Volume 84 of Advances in the Astronautical Sciences*, American Astronautical Society, April 1993
7. Goddard Space Flight Center, Flight Dynamics Division, 554-FDD-91/070R1UD0, *Multimission Three-Axis Stabilized Spacecraft (MTASS) Flight Dynamics Support System (FDSS) Functional Specifications Revision 1*, Jon Landis (CSC), prepared by Computer Sciences Corporation, September 1995
8. Computer Sciences Corporation (CSC), CSC/TM-77/6082, *Gyro Calibration Analysis for the High Energy Astronomy Observatory-A (HEAO-A)*, J. Keat, June 1977
9. J. Hashmall and D. Baker, "An Improved Transfer Function for the Fine Sun Sensor," presented at the International Symposium on Spaceflight Dynamics, sponsored by the Russian Space Academy, May 1994
10. W. Davis, J. Hashmall, A. Garber, H. Kang, and J. Zsoldos, "In-Flight Calibration of Alignment and Field of View Distortion for Spacecraft Attitude Sensors," Paper No. AAS 95-303, presented at the American Astronautical Society (AAS)/American Institute of Astronautics and Aeronautics (AIAA) Astrodynamic Specialists Conference, Halifax, Nova Scotia, August 1995

